ELSEVIER

Contents lists available at ScienceDirect

# Journal of Alloys and Compounds

journal homepage: www.elsevier.com/locate/jalcom



# Characteristic and function of the dynamic Al-AlN core-shell structure in Al-Al<sub>2</sub>O<sub>3</sub> composite at elevated temperature



Chenhong Ma a,b, Yong Li a, Peng Jiang a,\*, Yinan Shen a, M.A. Subramanian c, Shulong Ma d

- <sup>a</sup> School of Materials Science and Engineering, University of Science and Technology Beijing, Beijing 100083, China
- <sup>b</sup> Collaborative Innovation Center of Steel Technology, University of Science and Technology Beijing, Beijing 100083, China
- <sup>c</sup> Department of Chemistry, Oregon State University, Corvallis, OR 97330, USA
- <sup>d</sup> Beijing Tongda Refractory Technologies Co., Ltd., Beijing 100043, China

# ARTICLE INFO

Article history:
Received 14 March 2023
Received in revised form 11 May 2023
Accepted 22 June 2023
Available online 24 June 2023

Keywords: Al-Al<sub>2</sub>O<sub>3</sub> composite Al-AlN core-shell structure Microstructural analysis Sintering

# ABSTRACT

An Al-AlN core-shell structure with spatial confinement effect is set up in Al-Al $_2$ O $_3$  composite by prenitriding at 580 °C in flowing nitrogen. Its detailed characteristic and function evolution was examined over the temperature range from 600 °C to 1500 °C. With the temperature increase, the as formed Al-AlN coreshell structure in the composite undergoes two typical stages. First, from 660 °C to 900 °C, AlN shell is intact and serves as an "eggshell" to localize the molten Al core inside. When the temperature rises above 900 °C, AlN shell begins to crack under thermal stress, and the micronized Al cluster (mixture of droplets and vapor) was extracted out gradually. In this period, AlN shell serves as a slowly-released structure to control the gradual exposure of Al core and their conversion to highly-reactive micronized Al(1) and Al(g). On this basis, the controllable synthesis of AlN-based reinforcements can be realized by adjusting the nitriding path of Al with different states and scales. The detailed analysis of the dynamic Al-AlN core-shell structure at elevated temperature contributes to the better phase and morphology control of the Al-Al $_2$ O $_3$  composite for metallurgy.

© 2023 Published by Elsevier B.V.

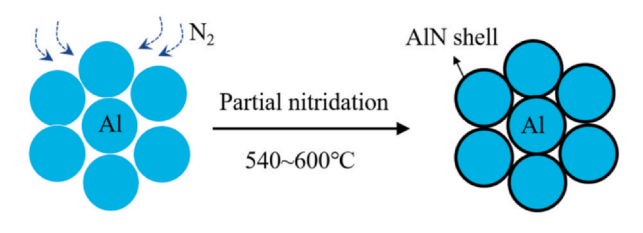
### 1. Introduction

AlN is an important non-oxide ceramic reinforcement for both lightweight aluminum (Al) based metal matrix composites (MMCs) [1–4] and traditional oxide ceramics [5–8]. AlN can be prepared by direct nitridation of metal Al powder. Direct nitridation has the advantage of low costs due to its simple reaction system and low reaction temperature [9,10]. However, aluminum powder is prone to melting and aggregation at the synthesis temperature, making it difficult for  $N_2$  gas to diffuse. And as the reaction progresses, the AlN layer formed on the surface of Al particles after nitriding also inhibits the diffusion of reactant  $N_2$  gas towards the unreacted Al at the center [10]. Therefore, for controllable direct nitridation, nitridation mechanisms of Al at different conditions have been studied carefully.

In the field of aluminum alloys, the direct nitridation of solid Al powder offers an in-situ and controllable synthesis route to expand the applications of Al-AlN MMCs and has been studied thereby

\* Corresponding author. E-mail address: jiangp@ustb.edu.cn (P. Jiang). [11–15]. Due to the low melting point of Al (660 °C), the partial nitridation of solid Al at 540–600 °C is employed, leading to a typical Al-AlN core-shell microstructure—an AlN shell enveloping the Al core (Fig. 1) [11–15]. The in-situ synthesis AlN shells form a rigid skeleton, which is proofed to offer more homogenous AlN distributions, and finer AlN cluster sizes of the AlN component and Al grain structure in the Al-AlN MMCs, which leads to better mechanical performance [11–13]. By establishing Al-AlN core-shell structure, Yu et al. prepared an in-situ formed AlN hollow sphere reinforced Al matrix syntactic foam parts by a subsequent "open-closed pore transformation" process [16].

Metal Al powder can also be used as a secondary phase to provide useful properties for traditional oxide ceramics or refractories. Al<sub>2</sub>O<sub>3</sub> is a typical oxide ceramic, which is widely used in electronics [17,18], machinery [19], chemical industry [20], automobile [21], metallurgy [22–24], aerospace [25], etc. These applications arise from its unique properties, such as chemical and thermal stability, relative strength, good wear resistance, high hardness, high melting point, good oxidation resistance, and good electrical and chemical resistance [25,26]. However, their applications are significantly restricted by brittleness and fabrication difficulties [26]. While the most crucial property for its high-temperature applications such as



Al power compact

Al-AlN core-shell structure

Fig. 1. Diagram of the typical Al-AlN core-shell structure in Al-AlN MMCs.

metallurgy is fracture toughness, i.e., the resistance to crack initiation and propagation. Improving fracture toughness and thermal shock resistance is therefore very important to extend the service life of Al<sub>2</sub>O<sub>3</sub> ceramics [26,27]. In the field of refractory materials for metallurgy, non-oxide ceramics with excellent fracture resistance, high thermal conductivity, and good compatibility with Al<sub>2</sub>O<sub>3</sub>, such as AlN, Al<sub>2</sub>OC-AlN solid solution, and AlON (aluminum oxynitride), are normally employed as reinforcing phases to enhance the fracture toughness and thermal shock resistance of the Al<sub>2</sub>O<sub>3</sub> ceramics [28–34]. Nitridation of Al-Al<sub>2</sub>O<sub>3</sub> composite compact shows better physical properties as the reinforcing non-oxide phases are in-situ formed and closely attached to the Al<sub>2</sub>O<sub>3</sub> particles [33–35]. The toughening and strengthening phase formed by in-situ reaction of Al in Al<sub>2</sub>O<sub>3</sub> matrix has fine grains and uniform microstructure, which presents particles, whiskers, plates and other microstructures depending on the conditions (temperature, atmosphere, etc.) [35–37]. This makes the composition and the structure designability on the micro scale of the Al<sub>2</sub>O<sub>3</sub> matrix composites more extensive, as well as its applications [38]. Previously, both complete nitriding of Al powder and uniform dispersion of the nitridation products in the Al<sub>2</sub>O<sub>3</sub> matrix are difficult to achieve as Al tends to aggregate and block pores due to its lower melting point than the vigorous nitridation temperature. Fig. 2(a) shows the microstructure of Al-Si-Al<sub>2</sub>O<sub>3</sub> composite directly nitrided at 1300 °C in nitrogen previously reported [39]. The bright colored area in Fig. 2(a) is metallic Al phase. which aggregates to form a continuous network as shown, hindering the complete and uniform nitridation of Al in the composite. As a result, only a small amount of AlN is generated, and most of the Al does not react and still exists in a free state in the composite [39]. Therefore, for technologies rely on the in-situ nitridation of Al-oxide composite at high temperatures, very limited information is available.

In our previous work, a novel two-step nitriding sintering of the  $Al-Al_2O_3$  composite refractories for metallurgy was proposed to successfully prepare  $Al_2OC-AlN$  solid solution reinforced  $Al_2O_3$  composite [40]. An Al-AlN core-shell structure was designed to

establish in the Al-Al<sub>2</sub>O<sub>2</sub> composite by nitriding at 580 °C (lower than melting point of Al) for 8 h, which localizes Al particles until it cracks at higher temperatures, thus solving the problem that the melting point of Al (660 °C) does not match the Al<sub>2</sub>OC-AlN solid solution generation temperature (> 1100 °C) [40]. The phase and microstructure evolution of the Al-AlN-Al<sub>2</sub>O<sub>3</sub> composite at high temperatures (1500–1700 °C) were carefully studied then [8,41]. By this two-step synthesis route, active AlN crystal seeds with multiple scales and morphologies are provided for Al<sub>2</sub>OC-AlN solid solution formation at different temperatures. As a result, under the spatial constraint effect of the Al-AlN core-shell structure, precise control of Al nitride products has been achieved. Fig. 2(b) shows the microstructure of Al-Si-Al<sub>2</sub>O<sub>3</sub> composite sample after two-step nitriding sintered at 1300 °C [32]. Compared with the directly nitrided sintered sample, the aluminum in the two-step nitrided sample has not aggregated into a continuous network and has been completely transformed into non-oxide reinforcing phases, which is attributed to the effect of Al-AlN core-shell structure [32]. Generally, the final properties of an Al-Al<sub>2</sub>O<sub>3</sub> composite product are highly dependent on the non-oxide phases and microstructure formed by reactions involving Al at high temperatures. While the reactions of Al at high temperatures are highly controlled by Al-AlN core-shell structure formed by solid Al nitridation. Therefore, it is expected to realize effective control of Al reaction mechanism at high temperatures through the spatial confinement effect of Al-AlN core-shell structure.

However, the Al-AlN core-shell structures are supposed to form through pre nitriding at low temperature (580 °C, below the melting temperature of Al), and will be fully consumed to transform to high temperature stable Al<sub>2</sub>OC-AlN solid solution or AlON in Al<sub>2</sub>O<sub>3</sub>. Therefore, they are never observed from the final products of Al-Al<sub>2</sub>O<sub>3</sub> samples nitrided at high temperatures (1300–1700 °C) in previous works [8,32,39–41]. The mechanism of spatial confinement effect of Al-AlN core-shell structure is still unclear. Their existence, morphology and further phase evolution were crucial to the control of the AlN based non-oxide reinforcements formation. Therefore, in this work, an Al-Al<sub>2</sub>O<sub>3</sub> composite sample with 12 wt% Al powder was prepared, an Al-AlN core-shell structure was established by pre-nitriding at 580 °C. Then, a steady heating process was exerted on the sample to carefully study its phase/microstructure evolution from 600 °C to 1500 °C in flowing nitrogen.

# 2. Experimental

In order to meet the performance requirements of functional refractories for continuous casting, tabular alumina (99.6%) with different particle sizes and Al powder ( $\leq$  45 µm, 99.3%) were used as raw material, and thermosetting phenolic resin was used as a binding agent. The chemical composition of the raw materials was

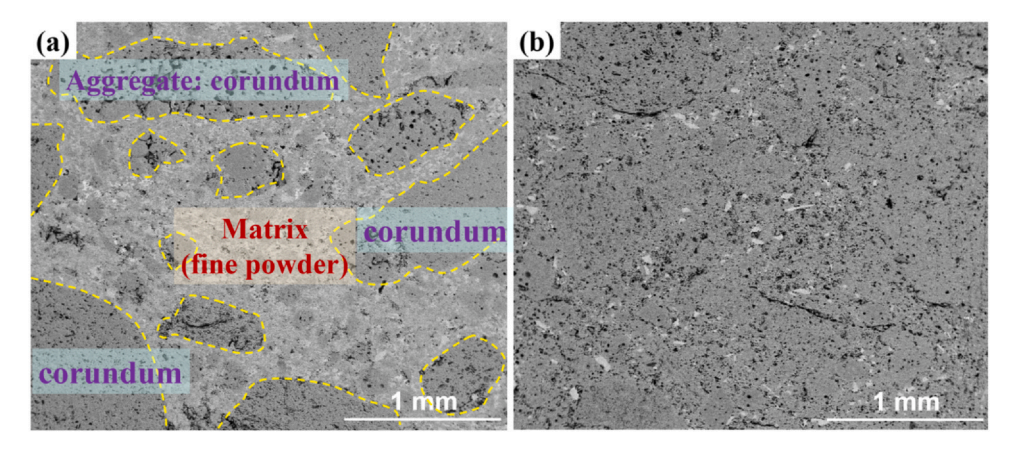


Fig. 2. Microstructure of Al-Si-Al<sub>2</sub>O<sub>3</sub> composite sample: (a) directly nitrided at 1300 °C, (b) two-step nitrided at 1300 °C [32,39].

**Table 1** Chemical analysis results of raw materials.

| Tabular alumina  | $Al_2O_3$   | Na <sub>2</sub> O | SiO <sub>2</sub> | Fe <sub>2</sub> O <sub>3</sub> | IL         |
|------------------|-------------|-------------------|------------------|--------------------------------|------------|
| wt%<br>Al powder | 99.42<br>Al | 0.31<br>Fe        | 0.16<br>Si       | 0.05                           | 0.06<br>IL |
| wt%              | 99.78       | 0.10              | 0.04             | ,                              | 0.08       |

**Table 2** Formulation of the Al-Al<sub>2</sub>O<sub>3</sub> composite sample (wt%).

| Sample | Tabular alumina |        |        | Al powder | Phenolic resin |
|--------|-----------------|--------|--------|-----------|----------------|
|        | 3–1 mm          | 1-0 mm | 5–0 μm | ≤ 45 μm   | extra          |
| S0     | 57              | 13     | 18     | 12        | 3.5            |

tested by X-ray fluorescence spectrometric method (Bruker, Germany, S2 PUMA Series II). Chemical analysis results of raw materials are illustrated in Table 1. The formulation of Al-Al<sub>2</sub>O<sub>3</sub> composites is shown in Table 2. The raw materials were mixed in an inclined mixer (German EIRICH Erich powerful mixer, R16W). First, the Al<sub>2</sub>O<sub>3</sub> granular aggregates were added in the mixer and mixed for 5 min, then the binder was added and further mixed for 5 min, finally the Al<sub>2</sub>O<sub>3</sub> and Al fine powders were added and further mixed for 15 min. The Al-Al<sub>2</sub>O<sub>3</sub> composite brick samples were obtained by compacting the mixed raw materials under 200 MPa using 630 t friction press (Qingdao Qing Forging and Forging Machinery Co., Ltd, China, J67Z-630).

The Al-Al $_2$ O $_3$  composite sample was heated at a heating rate of 10 °C/min to 580 °C and hold for 4 h with flowing nitrogen gas to establish an Al-AlN core-shell structure through Reaction (1). Then the sample with Al-AlN core-shell structure was further sintered from 600 °C to 1500 °C (3 °C/min) in 100 °C steps and hold for 3 h in flowing nitrogen, and then cooling with the furnace. The equipment used for sintering is an atmosphere sintering furnace (Model ZT-108-25 CH120816, Shanghai Chenhua Science Technology Corp., Ltd., China).

$$2AI(s) + N2(g) = 2AIN(s)$$
 (1)

Thermal gravimetry and differential scanning calorimetry (TG/DSC) of two different samples (with or without heat preservation at  $580\,^{\circ}\text{C}$  in  $N_2$ ) were studied in flowing nitrogen-gas up to  $1400\,^{\circ}\text{C}$  ( $10\,^{\circ}\text{C/min}$ ) using a thermal analyzer (Model STA 449F3, Netzsch, Selb, Germany). The phase and microstructure evolution of Al-Al<sub>2</sub>O<sub>3</sub> composite in the range of 580– $1500\,^{\circ}\text{C}$  were characterized by X-ray diffraction (XRD; Ultima IV Rigaku), scanning electron microscope (SEM) (Quanta FEG450, FEI) equipped with an energy-dispersive spectroscope (EDS) respectively to help understand the reaction

paths of Al in detail. The samples sintered at different temperatures were ball-milled into powders for XRD measurements. The XRD patterns were collected on a Rigaku instrument using Cu K $\alpha$  radiation (wavelength: 1.5415 nm). A scan speed of 5°/min in the continuous mode was applied, and the data were collected in a 2 $\theta$  range of 10–90°. The microstructure of the samples sintered at different temperatures was observed by SEM, and the micro selected area chemical composition quantitative analysis of the samples was studied using EDS. A gold coating was used to make the samples electrically conductive enough for SEM analysis.

#### 3. Results and discussion

#### 3.1. TG-DSC analysis

Fig. 3 shows the TG-DSC curve of  $Al-Al_2O_3$  composite samples with heat treatment at  $580\,^{\circ}C$  in nitrogen for  $4\,h$ , and the same composition without low temperature nitridation (green  $Al-Al_2O_3$  composite) was conducted for comparison.

An endothermic peak at 660 °C corresponding to aluminum melts and a maximum exothermic peak of its nitridation at 845 °C [Fig. 3(a)] appear in the DSC of the green Al-Al<sub>2</sub>O<sub>3</sub> composite. When Al-Al<sub>2</sub>O<sub>3</sub> composite is nitrided at 580 °C firstly, the maximum exothermic peak shifts to 931 °C [Fig. 3(b)], which is 86 °C higher than that of green Al-Al<sub>2</sub>O<sub>3</sub> composite. This is possible due to the fact that the AlN shell formed by pre nitriding at 580 °C protects the internal Al core from exposure to nitrogen in the lower temperature range. Weight changes of the green Al-Al<sub>2</sub>O<sub>3</sub> composite in the TG curve [Fig. 3(a)], include (i) the pyrolysis of phenolic resin binding agent from 150 °C to 600 °C and (ii) nitridation of aluminum between 800 °C and 900 °C. Above 900 °C, the weight of green Al-Al<sub>2</sub>O<sub>3</sub> composite sample does not increase apparently. A possible reason is that the large heat generated by the intensive reaction between Al and nitrogen leads to the coalescence of reactant Al particles, which is similar to the observation in Fig. 2(a), magnifying the difficulty of nitrogen diffusion. While, for the Al-Al<sub>2</sub>O<sub>3</sub> composite with Al-AlN core-shell structure, the weight increase includes two stages of (i) a fast increase from 900 °C to 950 °C and (ii) a slow increase from 950 °C to 1300 °C [Fig. 3(b)]. A reasonable explanation is that the cracking of Al-AlN core shell structure is gradual and sustainable with the increase of temperature. Accordingly, the exposure of fresh Al inside becomes less violent but proceed progressively, thus avoiding the accumulation of Al(1) and ensuring sustainable reaction between aluminum and N2, which is similar to what is shown in Fig. 2(b).

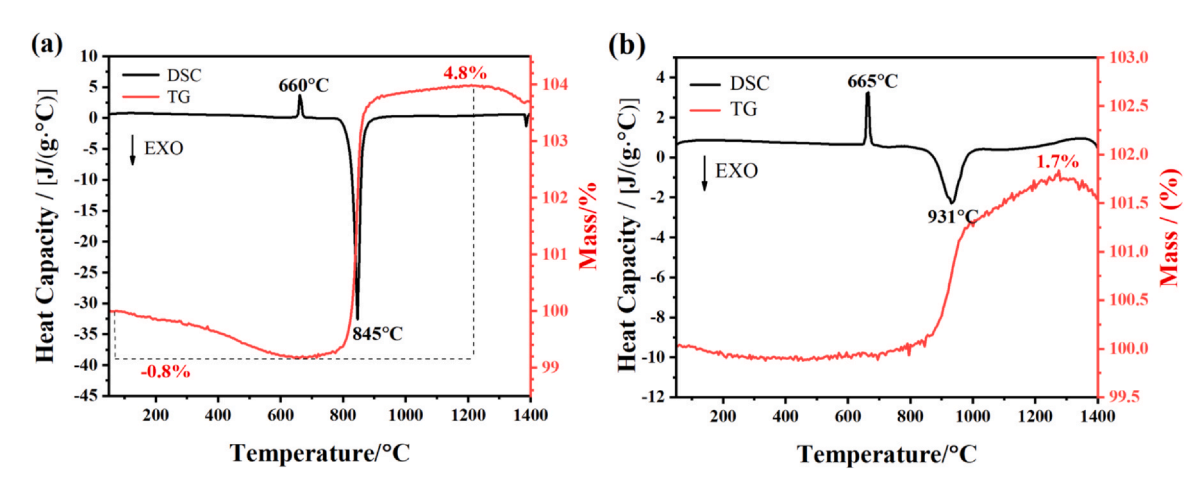


Fig. 3. TG-DSC curves of (a) green Al-Al<sub>2</sub>O<sub>3</sub> composite and (b) Al-Al<sub>2</sub>O<sub>3</sub> composite after nitridation at 580 °C in a flowing nitrogen-gas atmosphere.

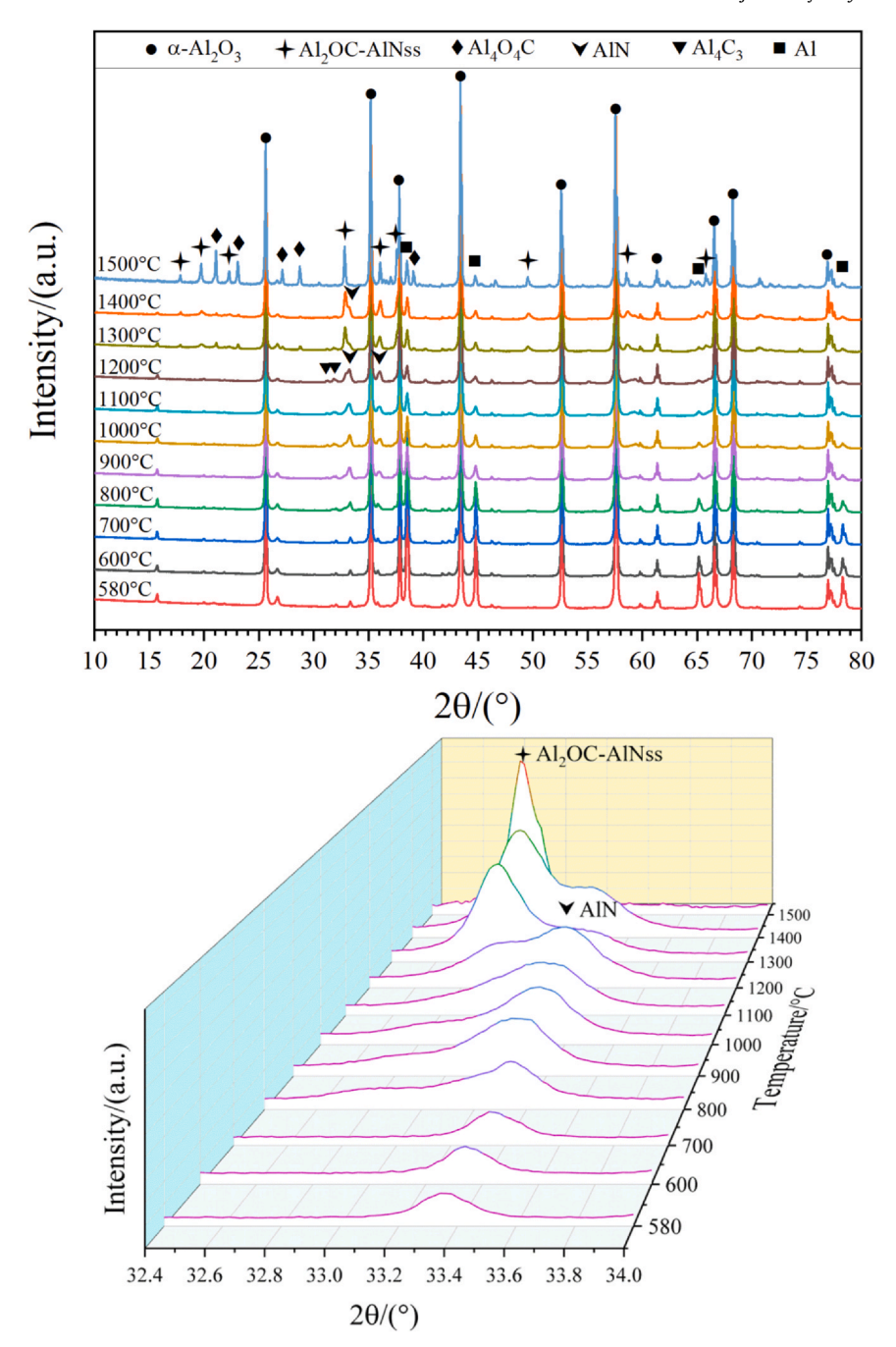


Fig. 4. XRD patterns of the Al-Al<sub>2</sub>O<sub>3</sub> composite sample pre nitrided at 580 °C and then sintered from 600 °C to 1500 °C in 100 °C steps with N<sub>2</sub> flowing.

# 3.2. Phase composition and Microstructure evolution analysis

Fig. 4 shows the phase evolution of  $Al-Al_2O_3$  composite which is pre nitrided at 580 °C and then sintered at evaluated temperatures from 600 °C to 1500 °C in the flowing nitrogen gas. As seen in Fig. 4, after pre-nitriding at 580 °C for 4 h, AlN peaks are detected in the  $Al-Al_2O_3$  composite sample, indicating the occurrence of nitridation of Al particles. For the samples further sintered at evaluated temperatures from 600 °C to 800 °C, the patterns did not change apparently, indicating a steady AlN content in the composite. This is attributed to the formation of a protective AlN layer on the surface of aluminum particle which inhibits the diffusion of the reactant nitrogen gas to the unreacted aluminum core. The nitriding reaction of Al particle with  $N_2$  is hard to proceed continuously at this stage,

since the diffusion coefficient of nitrogen in the nitrided layer is exclusively small.

When sintered at 900 °C for 3 h, the intensity of AlN peaks increased distinguishably. It is due to the fact that when the temperature is as high as 900 °C, Al-AlN core-shell structure in the composite begins to crack, which is mainly attribute to the mismatch of thermal expansion coefficient between AlN shell  $(4.5 \times 10^{-6} \, ^{\circ}\text{C}^{-1})$  and metal Al core  $(23 \times 10^{-6} \, ^{\circ}\text{C}^{-1})$  [42] and the inner impetus coming from Al vapor. According to Reaction (2) and the relevant thermodynamic data, the equilibrium pressure of Al(g)  $(P_{AI})$ was plotted as a function of temperature in Fig. 5. As shown in Fig. 5, the  $P_{AI}$  increases with temperature elevation. The  $P_{AI}$  at 660 °C is  $10^{-12.34}$  MPa, while the  $P_{AI}$  is  $10^{-8.85}$  MPa when the temperature is raised to 900 °C, which is an increase of 3–4 orders of magnitude. Thus, under the synergistic effect of thermal expansion of Al(1) and drive force of

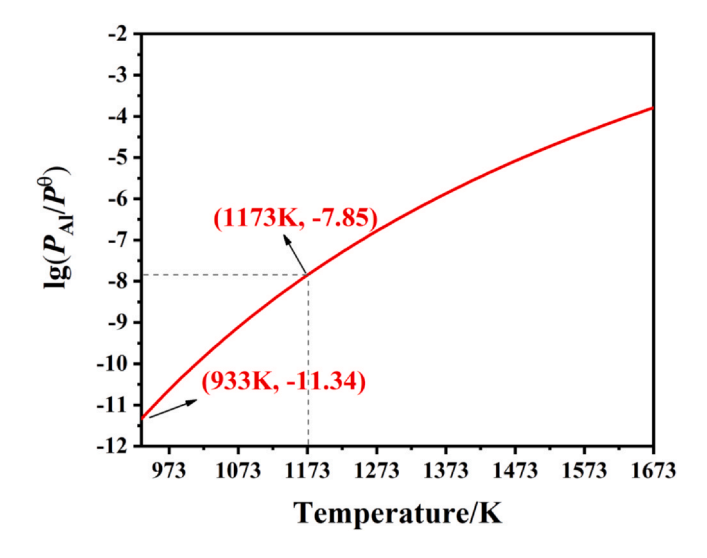


Fig. 5. Equilibrium pressure of Al vapor as a function of temperature.

Al(g), AlN shell cracks at about 900 °C. The TG-DSC curve [Fig. 3(b)] indicates that the apparent crack of Al-AlN core shell structure in the composite occurred at 931 °C. When sintered at temperature 900–1200 °C, the intensity of AlN peaks is positively correlated with temperature. Combined with the TG curve [Fig. 3(b)], it is believed that the fracture of Al-AlN core-shell structure above 900 °C is gradual with temperature increase. As a result, fresh Al clusters are continuously released and nitrided at elevated temperature, thus avoiding the aggregation of Al(l), forming AlN grains with multiscale and multi-morphologies.

$$Al(1) = Al(g) \quad \Delta G = 304640 - 109.50T + RT \ln(P_{Al}/P^{\theta})$$
 (2)

When sintered at 1200 °C, Al<sub>2</sub>OC-AlN solid solution phase was detected in the sample, and its content ratio sharply rose with the fully formation took place at 1500 °C. The growth mechanism of Al<sub>2</sub>OC-AlN solid solution reinforcement phase has been elaborated in detail in our previous work, it is that the isostructural AlN crystal nucleus from AlN shell served as crystal nuclei to reduce the potential barrier to be overcome for its synthesis, and the morphology of Al<sub>2</sub>OC-AlN solid solution mainly depends on the dynamic AlN mesophase [40]. While this work mainly explores the evolution mechanism of Al-AlN core shell structure in detail.

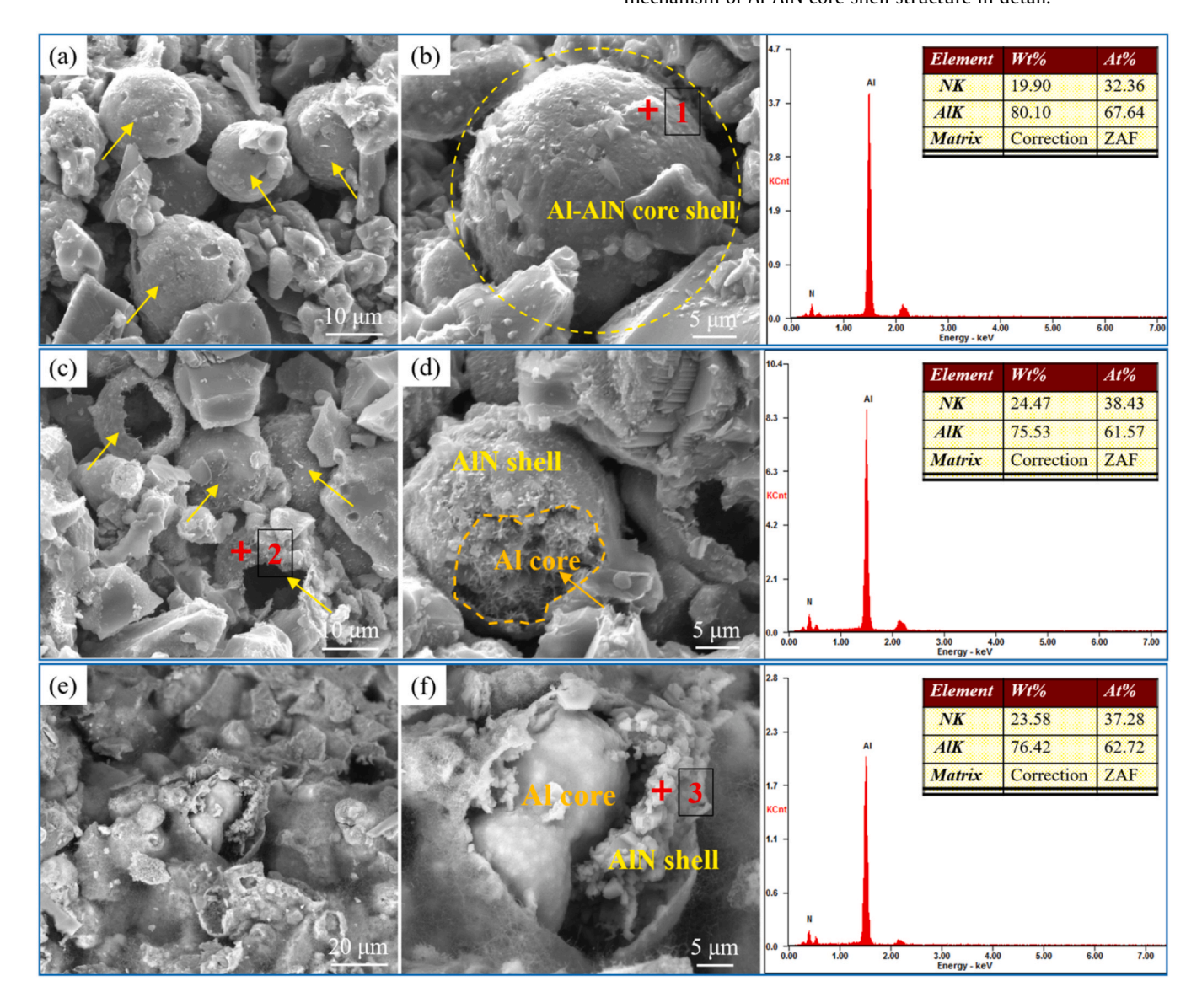


Fig. 6. SEM images and EDS analysis results of dynamic Al-AlN core-shell structure in Al-Al<sub>2</sub>O<sub>3</sub> composite sample (a, b) heat-treated at 580 °C and then sintered at (c, d) 800 °C and (e, f) 900 °C.

Fig. 6 shows the morphologies and EDS analysis results of the Al-AlN core-shell structure in Al-Al<sub>2</sub>O<sub>3</sub> composite sample at 580 °C, 800 °C and 900 °C, respectively. As shown in Fig. 6(a-b) and the corresponding EDS analysis result, the AlN layer formed at 580 °C consisting of nano-crystallites encapsulate Al particles, forming an Al-AlN core-shell structure successfully. As shown in Fig. 6(c), after sintered at 800 °C for 3 h, only a few Al-AlN core shell structures were slightly cracked, and the internal Al core was almost not exposed [Fig. 6(d)]. It proves that when the temperature is beyond the melting temperature of Al (660 °C), the Al core was melted while the AlN shell remained intact. The stability of Al-AlN core shell structure at temperature range from 660 °C to 900 °C is very crucial to the reaction efficiency and path of Al at subsequent high temperature sintering, as the melting point of aluminum is 660 °C while its violent nitriding reaction temperature is about 845 °C as confirmed by the TG-DSC curve. As shown in Fig. 6(e) and (f), when the temperature reaches 900 °C, a large amount of Al-AlN core shell structure were cracked, fresh Al core was released and exposed to N2 gas, thus allowing the further nitridation of Al as the violent reaction of Al has been reached. According to the EDS analysis, the shell formed on the surface of Al particles is mainly composed of Al and N elements, but the ratio between the detected Al and N is higher than 1:1 in AlN. It is due to the fact that the penetration depth  $(2-5 \mu m)$ into the sample), is bigger than the thickness of the AIN shell (less than 2 µm, as observed by SEM in Fig. 6(f). Therefore, some of the signals are actually collected from the internal Al core. The microstructure evolution observed by SEM and the EDS analysis results are consistent with the XRD and TG-DSC results.

Fig. 7 shows the Al-AlN core shell structure cracked in different degree at 900 °C. As seen from Fig. 7, the unbroken, slightly broken and completely broken Al-AlN core-shell structures coexist in the composite. This result shows that the dynamic Al-AlN core shell structure in the composite acts as a slow-control releasing agent during sintering or high-temperature service, sustaining the reaction of Al and realizing the controllable composition and morphology of reaction products.

Fig. 8 shows the morphology and EDS-Mapping analysis result of Al-AlN core shell structure in the sample sintered at  $1200\,^{\circ}$ C. As shown in Fig. 8(a), the spherical AlN shell distributes independently in the 3D network, and a good interfacial bonding between the  $Al_2O_3$  matrix and the in situ formed spherical AlN shell is obtained [Fig. 8(b)], which is considered to be conducive to the mechanical

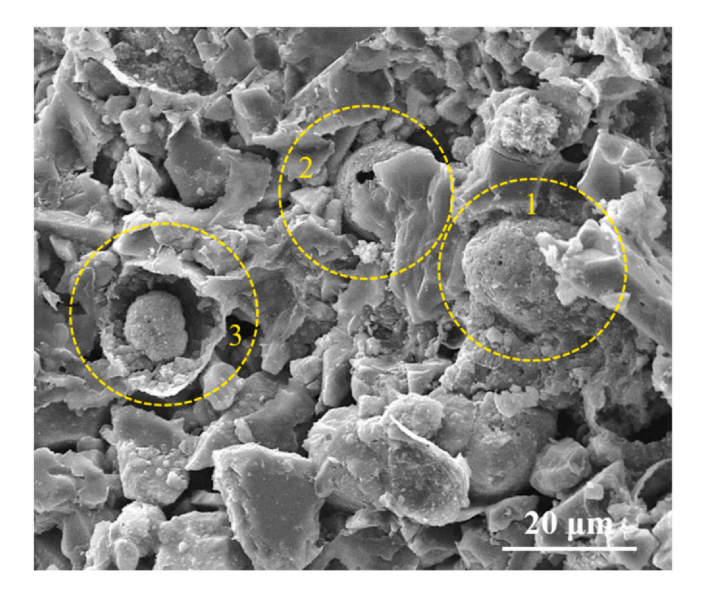


Fig. 7. SEM image of dynamic Al-AlN core-shell structures with different crack degrees at 900 °C.

strength of the material. The typical spherical AlN shell consisted of nano/micro-scale AlN crystals has a thickness of  $\sim 1.5\,\mu m$ , and the inner part of the shell is filled with whisker reaction products [Fig. 8(c)]. Fig. 8(d) shows the EDS-Mapping analysis of the Al-AlN core shell structure, which confirmed the formation of AlN shell. In addition to the pinning and bridging effect, this AlN dispersoids with typical spherical-shell-like microstructure is expected to improve the thermal shock resistance of the composite material due to its good thermal conductivity ( $\sim 210\,W\,m^{-1}\,K^{-1}$ ), which is much higher than that of Al<sub>2</sub>O<sub>3</sub> ( $\sim 30\,W\,m^{-1}\,K^{-1}$ ).

3.3. Analysis of evolution of Al-AlN core-shell structure in the Al-Al<sub>2</sub>O<sub>3</sub> sample with temperature

Based on the above results, the characteristic and function evolution of the dynamic Al-AlN core shell structure in  $Al-Al_2O_3$  composite refractories with temperature increasing is reasonably divided into two stages, as shown in Fig. 9.

Initially, an AlN layer is formed on the surface of aluminum particles by direct nitridation at 580 °C via V-S reaction mechanism (slightly lower than the melting point of aluminum). It could be treated as "zero" reaction rate as the reactants-Al core and nitrogengas are effectively separated by the formed nitride layer. Thus, a typical yolk-shell-like microstructure of metallic Al core and AlN shell is formed. In the first stage (660-900 °C), the Al core is melted while the AlN shell remains intact, which is attributed to the high coefficient of thermal expansion of AlN. Thus, the liquid Al particles are localized inside the AIN shell to prevent their aggregation at lower temperatures and exhibit dynamic reaction activity at high temperatures. It is through establishment of Al-AlN core shell structure with a good thermal stability that the high dispersion of molten Al particles in the matrix can be achieved, which is crucial to the transformation of Al into non-oxide reinforcements of Al<sub>2</sub>O<sub>3</sub> refractories.

In the second stage (> 900 °C). The AlN shell become crack under thermal stress and portion of Al clusters (Al droplet and Al vapor) is extracted out gradually. The driving force is possibly due to capillarity, surface tension of Al melt and inner impetus coming from Al vapor. The reaction mechanisms of Al in the composites depend appreciably on the morphology and integrity of the AIN shell, which is related to the heating rate of the particles and the thickness of AIN shell. When the heating rate is relatively slow, particles are usually able to maintain their integrity [43]. The AlN shell undergoes a degree of physical cracking, which provides fast channels for species to diffuse through, thereby resulting in different reaction rate controlling steps including the diffusion-controlled mechanism and the kinetic controlled mechanism [43-45]. When the heating is extremely fast, the particle may spall, which was described by the melt dispersion mechanism [43]. The solid AlN shell ruptures when the stress exerted due to the expansion of the melting aluminum core reaches a certain level. As shown in Fig. 7, the Al-AlN core shell structure with a very thin AIN shell or there are weak points in its nitride shell would preferentially crack. In contrast, the Al-AlN coreshell structure with a strong nitride layer cracked later at a higher temperature. The high pressure generates unloading waves and tensile forces to disperse the Al core into a multitude of micro-finer, dispersed Al clusters (including liquid Al droplets and Al vapor) [43]. Then, heterogeneous nitridation of smaller Al droplets leads to new micronized Al-AlN core-shell structures formation, which cracks with the increase of temperature and much finer, dispersed Al clusters are split out. With the dynamic splitting of the Al-AlN coreshell structures, finer micro and nano Al particles with high surfaceto-volume ratio is dispersed in the composite, and leading to a higher thermodynamic equilibrium Al vapor pressure. According to Reaction (2) and Kelvin equation (3), the Al vapor partial pressure of Al droplet with different particle size at 1200 °C is calculated and

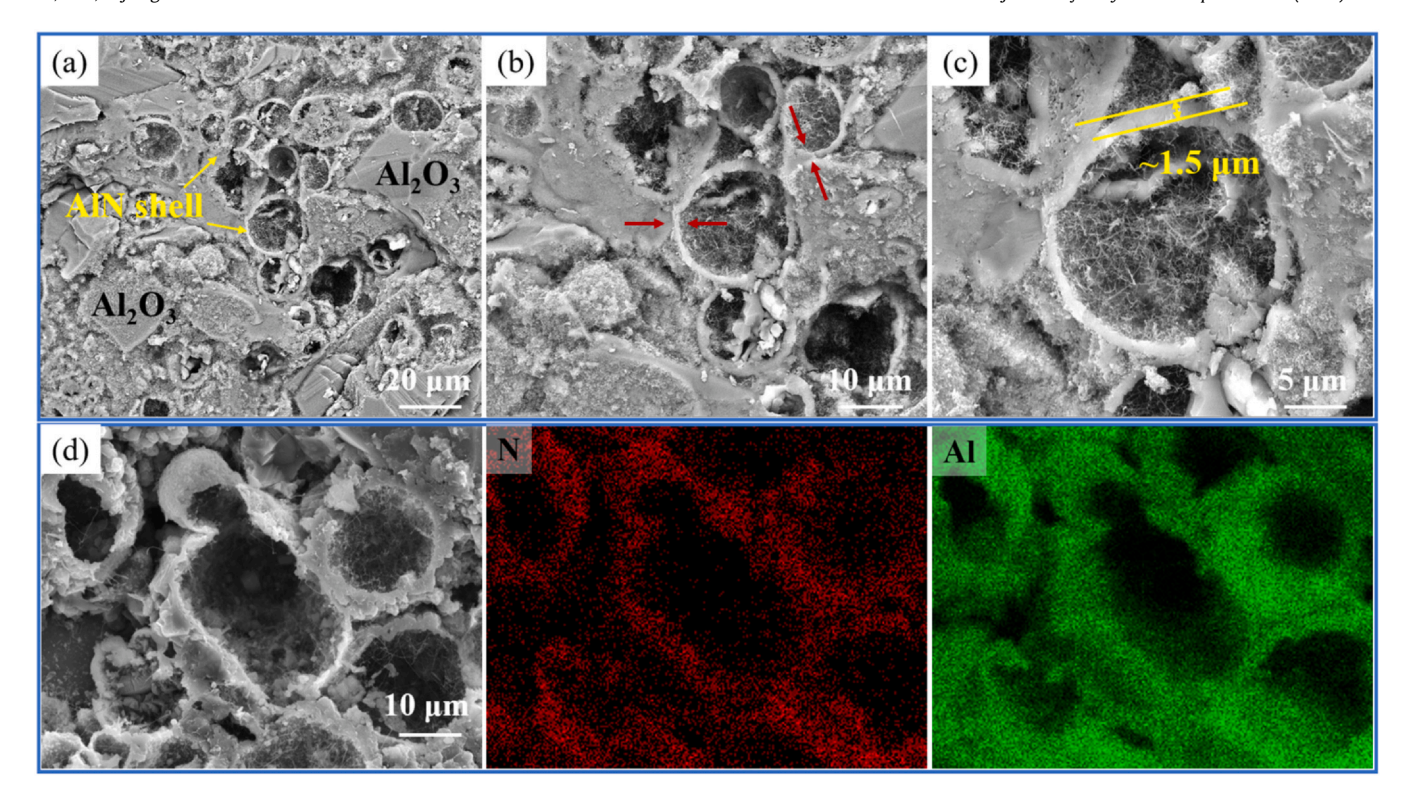


Fig. 8. SEM images and EDS-Mapping analysis of Al-Al<sub>2</sub>O<sub>3</sub> composite sample sintered at 1200 °C in flowing nitrogen gas.



Fig. 9. Formation and evolution of dynamic Al-AlN core shell structure at evaluated temperature.

**Table 3** The Al vapor partial pressure of Al droplet with different particle size at  $1200\,^{\circ}$ C.

| r/m              | 10 <sup>-6</sup> (1 μm)  | 10 <sup>-7</sup>         | 10 <sup>-8</sup>         | 10 <sup>-9</sup> (1 nm)  |
|------------------|--------------------------|--------------------------|--------------------------|--------------------------|
| P/P <sub>0</sub> | 1.001                    | 1.012                    | 1.131                    | 3.421                    |
| P <sub>Al</sub>  | 8.136 × 10 <sup>-7</sup> | 8.226 × 10 <sup>-7</sup> | 9.193 × 10 <sup>-7</sup> | 2.781 × 10 <sup>-6</sup> |

listed in Table 3. The whisker-like products shown in Fig. 8 is considered to be generated by the gas-phase reaction involving Al vapor.

$$ln \frac{P}{P_0} = \frac{2\sigma M}{\rho RTr} \tag{3}$$

Where r is the radius of the droplet, M is the molecular weight of liquid,  $\rho$  is the density of liquid, T is the temperature,  $\sigma$  is surface tension of liquid, R is the gas constant,  $P_0$  is the vapor pressure of a

liquid when the surface is flat, and P is the vapor pressure of droplets with radius r.

Both micronized liquid Al particles and Al vapor have high reactive activity, which boosts the reaction rate. Moreover, the composition and morphology of reaction products largely depend on the form (vapor or liquid) and scale (micron or nanometer) of the reactant Al. By controlling the reaction path of Al through dynamic Al-AlN core-shell structure, controllable products and microstructure is expected to be achieved.

Base on the above results, it is believed that through establishment of Al-AlN core shell structure, the problem that the low melting point of aluminum does not match the reaction temperature or service temperature of refractories has been successfully solved. Fig. 10 illustrates the microstructure evolution of Al-Al<sub>2</sub>O<sub>3</sub> composite sample with Al-AlN core-shell structure during sintering. It is

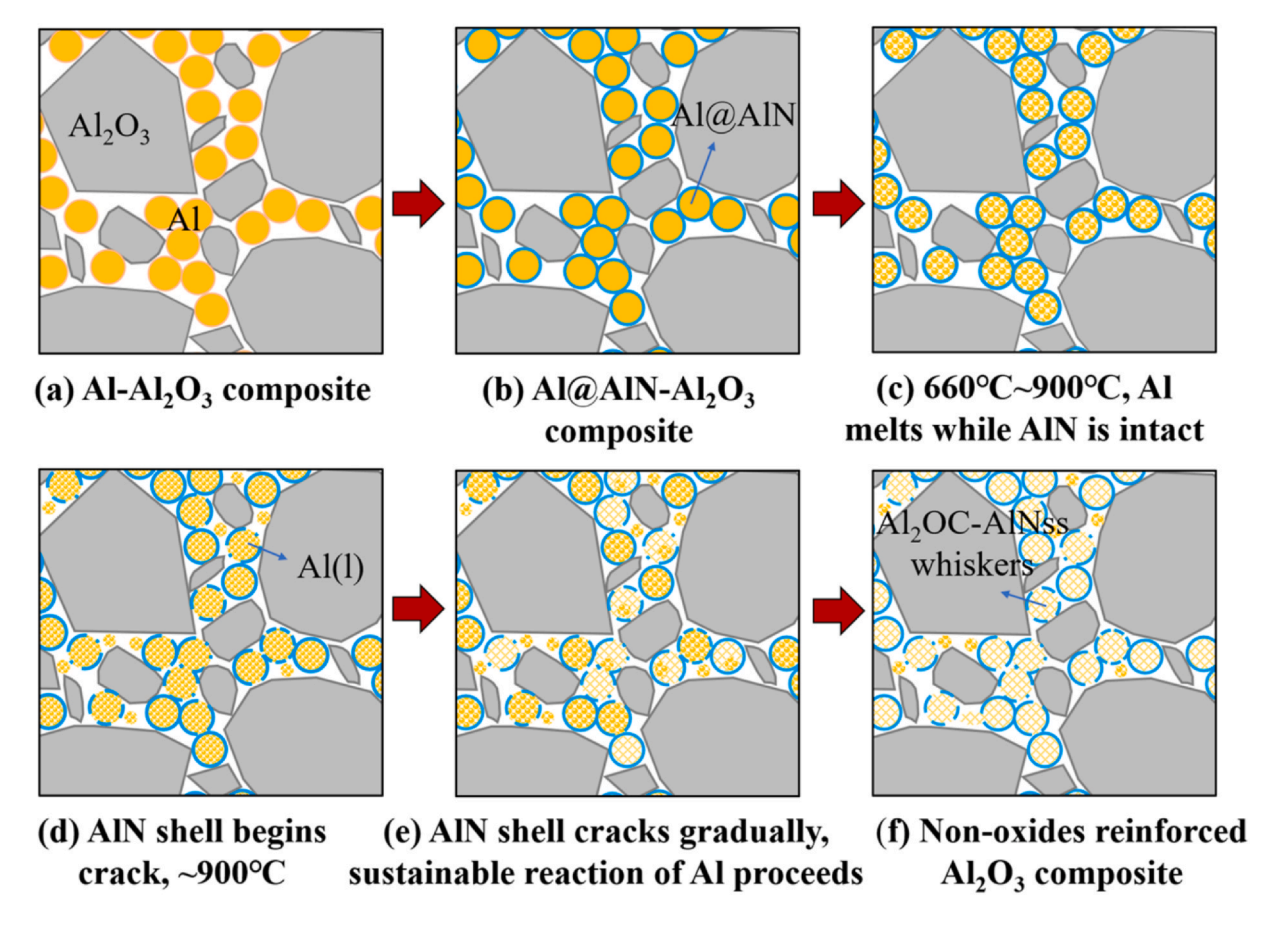


Fig. 10. Evolution of Al-Al<sub>2</sub>O<sub>3</sub> composite sample at evaluated temperature.

expected to provide a favorable guidance for the high-temperature application of  $Al-Al_2O_3$  composite refractories, as well as any other aluminum-oxide composite materials.

# 4. Conclusion

Dynamic Al-AlN core shell structure has been formed in situ in the Al-Al<sub>2</sub>O<sub>3</sub> composite by pre nitriding at 580 °C in flowing nitrogen-gas. It is critical for successful transformation of Al into a non-oxide reinforcing phase during high temperature sintering or service, since it prevents the accumulation of Al melt and ensures the sustainable high-temperature reaction of Al. The XRD and SEM results indicated that the Al-AlN core shell structure were stable at the temperature range from 660 °C to about 900 °C, so that the localization of Al melt before reaching the violent reaction temperature of Al can be achieved. When above 900 °C, AlN shell began to crack and micronized Al cluster (Al droplets and vapor) was extracted out gradually, and this process proceed sustainably with temperature increasing. Through this sustainable process of slowly and gradually releasing Al droplets with smaller size and Al vapor in the system controlled by dynamic Al-AlN core shell structure, controllable reaction path of Al at high temperatures and the resulting reaction products and microstructure can be achieved. The detailed analysis of the dynamic Al-AlN core-shell structure at elevated temperature contributes to the better phase and morphology control of the Al-Al<sub>2</sub>O<sub>3</sub> composite for metallurgy.

# **CRediT authorship contribution statement**

**Chenhong Ma:** Data curation, Writing – original draft, Conceptualization, Methodology. **Yong Li:** Visualization,

Investigation, Writing – original draft. **Peng Jiang:** Conceptualization, Writing – review & editing, Supervision. **Yinan Shen:** Software. **M. A. Subramanian:** Writing – review & editing. **Shulong Ma:** Data curation.

#### **Data Availability**

Data will be made available on request.

# **Declaration of Competing Interest**

The authors declare that they have no known competing financial interests or personal relationships that could have appeared to influence the work reported in this paper.

# Acknowledgements

This work was supported by the National Key Research and Development Program of China (2021YFB3701400) and Youth Teacher International Exchange & Growth Program under the Grant no. QNXM20220018. The work done at Oregon State University is supported by US National Science Foundation Grant no. DMR-2025615. Thank you for the support and assistance by Innovation Center of Beijing Association for Science and Technology in this project.

#### References

[1] K.B. Lee, S.H. Kim, D.Y. Kim, P.R. Cha, H.S. Kim, H.J. Choi, J.P. Ahn, Aluminum matrix composites manufactured using nitridation-induced self-forming process, Sci. Rep. 9 (1) (2019) 20389, https://doi.org/10.1038/s41598-019-56802-3

- [2] D. Kent, G.B. Schaffer, T.B. Sercombe, J. Drennan, A novel method for the production of aluminium nitride, Scr. Mater. 54 (12) (2006) 2125–2129, https://doi.org/10.1016/j.scriptamat.2006.02.047
- [3] J. Kim, J. Park, C.H. Shim, J.P. Ahn, H. Choi, K.B. Lee, Preparation of Al/AlN composites by in-situ reaction in the nitridation-induced self-forming process, J. Compos. Mater. 56 (24) (2022) 3653–3658, https://doi.org/10.1177/0021988232119371
- [4] H. Jang, S.H. Kim, N. Lee, P.R. Cha, J.P. Ahn, H. Choi, K.B. Lee, Mechanism for self-formation of Al matrix composites using nitridation-induced manufacturing processes, J. Mater. Res. Technol. 18 (2022) 2331–2342, https://doi.org/10.1016/j.jmrt.2022.03.130
- [5] J. Liu, J. Binner, R. Higginson, Z. Zhou, Interfacial reactions and wetting in Al-Mg/ oxide ceramic interpenetrating composites made by a pressureless infiltration technique, Compos. Sci. Technol. 72 (8) (2012) 886–893, https://doi.org/10.1016/ i.compscitech.2012.02.018
- [6] X. Wu, Y. Li, P. Jiang, J. Sun, In situ formation mechanism of spinel-like Al<sub>2</sub>O<sub>6</sub>N and plate-like Al<sub>2</sub>O<sub>3</sub>N<sub>5</sub> in the two-step sintered Al-Al<sub>2</sub>O<sub>3</sub> composites, Mater. Chem. Phys. 271 (2021) 124951, https://doi.org/10.1016/j.matchemphys.2021. 124951
- [7] M. Yang, G. Xiao, D. Ding, Y. Yang, M. Jiang, D. Yang, S. Yuan, In situ formation mechanism of aluminum oxycarbonitride in the unoxidized zone of Al-Al<sub>2</sub>O<sub>3</sub> composites, Ceram. Int. 47 (16) (2021) 22949–22956, https://doi.org/10.1016/j. ceramint 2021.05.008
- [8] X. Wu, Y. Li, C. Ma, P. Jiang, J. Sun, Study on phase evolution of the resin bonded Al-Al<sub>2</sub>O<sub>3</sub> composites in N<sub>2</sub>-flowing at high temperature, J. Alloy. Compd. 784 (2019) 1145–1152, https://doi.org/10.1016/j.jallcom.2019.01.054
- [9] L. Jia, K. Kondoh, H. Imai, M. Onishi, B. Chen, S.F. Li, Nano-scale AlN powders and AlN/Al composites by full and partial direct nitridation of aluminum in solidstate, J. Alloy. Compd. 629 (2015) 184–187, https://doi.org/10.1016/j.jallcom. 2014.12.220
- [10] T. Okada, M. Toriyama, S. Kanzaki, Synthesis of aluminum nitride sintered bodies using the direct nitridation of Al compacts, J. Eur. Ceram. Soc. 20 (6) (2000) 783–787, https://doi.org/10.1016/S0955-2219(99)00204-6
- [11] M. Balog, P. Yu, M. Qian, M. Behulova, P. Svec Sr, R. Cicka, Nanoscaled Al-AlN composites consolidated by equal channel angular pressing (ECAP) of partially in situ nitrided Al powder, Mater. Sci. Eng.: A 562 (2013) 190–195, https://doi.org/10.1016/j.msea.2012.11.040
- [12] P. Yu, M. Balog, M. Yan, G.B. Schaffer, M. Qian, In situ fabrication and mechanical properties of Al-AlN composite by hot extrusion of partially nitrided AA6061 powder, J. Mater. Res. 26 (14) (2011) 1719–1725, https://doi.org/10.1557/jmr. 2011 143
- [13] T.B. Sercombe, G.B. Schaffer, Rapid manufacturing of aluminum components, Science 301 (5637) (2003) 1225–1227 (https://www.science.org/doi/full/10.
- [14] T.B. Sercombe, G.B. Schaffer, On the role of tin in the infiltration of aluminium by aluminium for rapid prototyping applications, Scr. Mater. 51 (9) (2004) 905–908, https://doi.org/10.1016/j.scriptamat.2004.06.032
- [15] T.B. Sercombe, G.B. Schaffer, On the role of tin in the nitridation of aluminium powder, Scr. Mater. 55 (4) (2006) 323–326, https://doi.org/10.1016/j.scriptamat. 2006.04.045
- [16] P. Yu, M. Qian, Metal injection moulding of in-situ formed AlN hollow sphere reinforced Al matrix syntactic foam parts, Mater. Chem. Phys. 137 (2) (2012) 435–438, https://doi.org/10.1016/j.matchemphys.2012.09.044
- [17] R.H. French, Electronic band structure of Al<sub>2</sub>O<sub>3</sub>, with comparison to Alon and AlN, J. Am. Ceram. Soc. 73 (3) (1990) 477–489, https://doi.org/10.1111/j.1151-2916 1990 tb06541 x
- [18] V.V. Rao, M.K. Murthy, J. Nagaraju, Thermal conductivity and thermal contact conductance studies on Al<sub>2</sub>O<sub>3</sub>/Al–AlN metal matrix composite, Compos. Sci. Technol. 64 (16) (2004) 2459–2462, https://doi.org/10.1016/j.compscitech.2004. 05.009
- [19] D. Jianxin, L. Lili, L. Jianhua, Z. Jinlong, Y. Xuefeng, Failure mechanisms of TiB<sub>2</sub> particle and SiC whisker reinforced Al<sub>2</sub>O<sub>3</sub> ceramic cutting tools when machining nickel-based alloys, Int. J. Mach. Tools Manuf. 45 (12–13) (2005) 1393–1401, https://doi.org/10.1016/j.ijmachtools.2005.01.033
- [20] P. Zamani, Z. Valefi, K. Jafarzadeh, Comprehensive study on corrosion protection properties of Al<sub>2</sub>O<sub>3</sub>, Cr<sub>2</sub>O<sub>3</sub> and Al<sub>2</sub>O<sub>3</sub>-Cr<sub>2</sub>O<sub>3</sub> ceramic coatings deposited by plasma spraying on carbon steel, Ceram. Int. 48 (2) (2022) 1574–1588, https:// doi.org/10.1016/i.ceramint.2021.09.237
- [21] A. Okada, Ceramic technologies for automotive industry: current status and perspectives, Mater. Sci. Eng.: B 161 (1-3) (2009) 182-187, https://doi.org/10. 1016/i.mseb.2008.11.017
- [22] D.R. Larson, J.A. Coppola, D.P.H. Hasselman, R.C. Bradt, Fracture toughness and spalling behavior of high-Al<sub>2</sub>O<sub>3</sub> refractories, J. Am. Ceram. Soc. 57 (10) (1974) 417–421, https://doi.org/10.1111/j.1151-2916.1974.tb11372.x

- [23] C. Zhao, M. Yan, H. Li, Z. Niu, B. Liang, J. Shang, Recent progress on Al<sub>2</sub>O<sub>3</sub>-C refractories with low/ultra-low carbon content: a review, China's Refract. 31 (1) (2022) 35 (http://www.cnref.cn/EN/10.19691/j.cnki.1004-4493.2022.01.006).
- [24] X. Wang, C. Deng, J. Di, G. Xing, J. Ding, H. Zhu, C. Yu, Enhanced oxidation resistance of low-carbon MgO-C refractories with Al₃BC₃-Al antioxidants: a synergistic effect, J. Am. Ceram. Soc. 106 (2023) 3749–3764, https://doi.org/10.1111/jace.19023
- [25] P. Auerkari, Mechanical and Physical Properties of Engineering Alumina Ceramics 23 Technical Research Centre of Finland, Espoo, 1996.
- [26] J. Liu, H. Yan, K. Jiang, Mechanical properties of graphene platelet-reinforced alumina ceramic composites, Ceram. Int. 39 (6) (2013) 6215–6221, https://doi. org/10.1016/j.ceramint.2013.01.041
- [27] I. Ahmad, H. Cao, H. Chen, H. Zhao, A. Kennedy, Y.Q. Zhu, Carbon nanotube toughened aluminium oxide nanocomposite, J. Eur. Ceram. Soc. 30 (4) (2010) 865–873, https://doi.org/10.1016/j.jeurceramsoc.2009.09.032
- [28] C. Yu, Y. Zheng, G. Xing, J. Ding, H. Zhu, Z. Wang, J. Di, A novel strategy for the fabrication of AlN–AlON refractories: nitrogen gas pressure sintering of Al<sub>4</sub>O<sub>4</sub>C, J. Am. Ceram. Soc. 105 (12) (2022) 7111–7121, https://doi.org/10.1111/jace.18709
- [29] X. Wu, C. Deng, J. Di, J. Ding, H. Zhu, C. Yu, Fabrication of novel AlN-SiC-C refractories by nitrogen gas-pressure sintering of Al<sub>4</sub>SiC<sub>4</sub>, J. Eur. Ceram. Soc. 42 (8) (2022) 3634–3643, https://doi.org/10.1016/j.jeurceramsoc.2022.02.058
- [30] H. Qin, Y. Li, P. Jiang, W. Xue, S. Tong, M. Yan, In-situ synthesis of AlON reinforcing phases in resin bonded Al<sub>2</sub>O<sub>3</sub> composite materials, J. Alloy. Compd. 711 (2017) 1–7, https://doi.org/10.1016/j.jallcom.2017.03.211
- [31] Y.W. Kim, Y.W. Oh, S.Y. Yoon, R. Stevens, H.C. Park, Thermal diffusivity of reaction-sintered AlON/Al<sub>2</sub>O<sub>3</sub> particulate composites, Ceram. Int. 34 (8) (2008) 1849–1855, https://doi.org/10.1016/j.ceramint.2007.06.004
- [32] C. Ma, Y. Li, L. Zhang, W. Xue, J. Sun, Formation of (Al<sub>2</sub>OC)<sub>1−x</sub>(AlN)<sub>x</sub> solid solution starting from Al–Si–Al<sub>2</sub>O<sub>3</sub> powder matrix at 1300 °C in flowing nitrogen, J. Am. Ceram. Soc. 102 (10) (2019) 6349–6356, https://doi.org/10.1111/jace.16486
- [33] P. Jiang, J. Sun, W. Xue, J. Chen, R.V. Kumar, Y. Li, New synthetic route to Al<sub>4</sub>O<sub>4</sub>C reinforced Al–Al<sub>2</sub>O<sub>3</sub> composite materials, Solid State Sci. 46 (2015) 33–36, https://doi.org/10.1016/j.solidstatesciences.2015.05.006
- [34] X. Wu, P. Jiang, Y. Li, J. Sun, Study on the synthesis and formation mechanism of Al<sub>2</sub>OC-AlN solid solution in Al-Al<sub>2</sub>O<sub>3</sub> composite material in air at 1500 °C, Solid State Sci. 100 (2020) 106112, https://doi.org/10.1016/j.solidstatesciences.2019. 106112
- [35] Y. Sun, Y. Li, L. Zhang, Y. Shen, J. Sun, Synthesis of  $(Al_2OC)_{1-x}(AlN)_x$  whiskers via  $Al_2O(g)$  transient phase in  $Al-Al_2O_3$  composite at 1000-1300 °C in flowing  $N_2$ , J. Asian Ceram. Soc. 8 (3) (2020) 624–633, https://doi.org/10.1080/21870764.2020.
- [36] C. Ma, Y. Li, L. Zhang, P. Jiang, Y. Shen, Reaction bonding alumina with AlN–SiC solid solution by nitridation of matrix containing Al–Si powders, J. Mater. Sci. 54 (2019) 14654–14665, https://doi.org/10.1007/s10853-019-03959-x
- [37] C. Ma, Y. Li, P. Jiang, W. Xue, J. Chen, Formation mechanism of γ-AlON and β-SiC reinforcements in a phenolic resin-bonded Al-Si-Al<sub>2</sub>O<sub>3</sub> composite at 1700 °C in flowing N<sub>2</sub>, J. Mater. Sci. 55 (14) (2020) 5772–5781, https://doi.org/10.1007/s10853-020-014450-8
- [38] M. Hasan, J. Zhao, Z. Jiang, Micromanufacturing of composite materials: a review, Int. J. Extrem. Manuf. 1 (1) (2019) 012004(https://iopscience.iop.org/article/10. 1088/2631-7990/ah0f74/meta)
- [39] C. Ma, Study on the application performance of Al-Si-Al<sub>2</sub>O<sub>3</sub> composite refractory materials, Univ. Sci. Technol. Beijing (2022), https://doi.org/10.26945/d.cnki. gbiku.2022.000139
- [40] X. Wu, Y. Li, P. Jiang, J. Sun, Controllable synthesis of Al<sub>2</sub>OC-AlN solid solution by two-step sintering in resin-bonded Al-Al<sub>2</sub>O<sub>3</sub> composites, Mater. Chem. Phys. 241 (2020) 122410, https://doi.org/10.1016/j.matchemphys.2019.122410
- [41] M. Yan, Y. Li, H. Li, J. Sun, Theoretical analysis and synthesis of Al<sub>4</sub>O<sub>4</sub>C and Al<sub>2</sub>CO phase in the resin bonded Al-Al<sub>2</sub>O<sub>3</sub> refractory in N<sub>2</sub>-flowing, Ceram. Int. 44 (2) (2018) 1493–1499, https://doi.org/10.1016/j.ceramint.2017.10.060
- [42] A. Kalemtas, G. Topates, O. Bahadir, K.A.Y.A. Pinar, H. Mandal, Thermal properties of pressureless melt infiltrated AlN-Si-Al composites, Trans. Nonferrous Met. Soc. China 23 (5) (2013) 1304–1313, https://doi.org/10.1016/S1003-6326(13)
- [43] Y.A. Tang, C. Kong, Y.A. Zong, S.A. Li, J.A. Zhuo, Q.A. Yao, Combustion of aluminum nanoparticle agglomerates: from mild oxidation to microexplosion, Proc. Combust. Inst., vol. 36, 2017, pp. 2325–32. (https://doi.org/10.1016/j.proci.2016. 06 144)
- [44] S. Chowdhury, K. Sullivan, N. Piekiel, L. Zhou, M.R. Zachariah, Diffusive vs explosive reaction at the nanoscale, J. Phys. Chem. C 114 (20) (2010) 9191–9195, https://doi.org/10.1021/jp906613p
- [45] T. Bazyn, N. Glumac, H. Krier, T.S. Ward, M. Schoenitz, E.L. Dreizin, Reflected shock ignition and combustion of aluminum and nanocomposite thermite powders, Combust. Sci. Technol. 179 (3) (2007) 457–476, https://doi.org/10.1080/ 00102200600637261